18TH WORLD CONFERENCE ON EARTHQUAKE ENGINEERING
WCEE2024
MILAN

MILAN, ITALY
30TH JUNE - 5TH JULY 2024
www.wcee2024.it

IMPORTANCE OF HAZARD-CONSISTENT RECORD SELECTION FOR THE RISK ASSESSMENT OF NPP COMPONENTS

N. Šipčić[1], P. García de Quevedo Iñarritu[2], M.Kohrangi[3] & P. Bazzurro[2]

[1] University School for Advanced Studies IUSS, Pavia, Italy, nevena.sipcic@iusspavia.it

[2] University School for Advanced Studies IUSS, Pavia, Italy

[3] RED Risk Engineering + Development, Pavia, Italy

Abstract: *This study focuses on the seismic risk assessment of non-structural components within the reactor building of a nuclear power plant (NPP) and presents the case study of a water pump. We consider two variants of the pump: one with the fundamental period, T_1, of 0.1s and the other with T_1 of 0.25s. Our objective is to compare two approaches for computing fragility and response hazard curves, with a particular emphasis on the importance of ensuring consistency of the ground motions utilized to derive them with the seismic hazard at the site. The first approach involves utilizing records selected with the Conditional Spectrum (CS) method consistent with the hazard at ten intensity levels corresponding to return periods ranging from 42 to 50,000 years. The second approach involves employing Incremental Dynamic Analysis (IDA) and utilizing records where hazard consistency is not explicitly enforced. We investigate different conditioning intensity measures: peak ground acceleration (PGA), spectral acceleration at the fundamental period of the component (i.e., $Sa(T_1)$), and average spectral acceleration in an appropriate range of oscillatory periods (AvgSa). The former set of curves is appropriate for a site-specific NPP risk assessment study, whereas the latter can provide an indication of how a water pump at a generic site may respond to earthquake ground motions but is not suitable for a site-specific NPP safety assessment. As a case study, we selected a site located along the western coast of Tuscany, Italy. The hazard model is developed in OpenQuake, based on the European Seismic Hazard Model (ESHM20) seismogenic-source model. The reactor building and water pump are modeled in a simplified manner, using OpenSees software, and the selected records are then used to perform Nonlinear Response History Analysis (NLRHA). Fragility and response hazard curves for both considered cases are compared, highlighting the significance of hazard consistency in accurately assessing the seismic risk of components in the NPP.*

1. Introduction

The most commonly used method for assessing the seismic risk of NNPPs is Seismic Probabilistic Risk Assessment (SPRA) (EPRI, 2003), whose objective is to estimate the failure rate of a component or structure by combining the results of seismic hazard analysis with those of seismic fragility analysis. The former provides the likelihood of observing at the site ground motion intensity measures (IMs) in exceedance of increasing levels of severity in a given period of time. The latter establishes the chances that any given asset may reach a specific damage level or worse should it experience different levels of IMs. The threshold of each damage state is expressed in terms of an engineering demand parameter (EDP) being attained. Typically, a scalar IM is used to characterize ground motion shaking and a single EDP is used to monitor the response severity of a

structure or a component. Fragility curves, often derived analytically due to the lack of empirical data, require the IM-EDP relationship obtained through nonlinear response history analyses (NLRHA) using selected ground motion records (GMs). Record selection, therefore, serves as a critical link between seismic hazard and structural response, emphasizing the need to judiciously select sets of ground motions, statistically consistent with those that may be observed at the site of interest.

The importance of hazard consistency has been highlighted many times in the past years. Methods such as the Conditional Mean Spectrum (CMS) (Baker, 2011), and, more comprehensively, the Conditional Spectrum (CS) (Jayaram et al., 2011) have been proposed for this purpose. These methodologies involve the selection and scaling of GMs to match the entire conditional distribution of spectral accelerations (Sa) expected at the site and intensity level of interest. This process ensures that the mean (in the case of CMS) and also the variance (in the case of CS) of the selected set of GMs are consistent with the hazard. This approach can be extended to include characteristics of the ground motion other that spectral acceleration that might be relevant (e.g., Bradley, 2010; Chandramohan et al., 2016). CMS or CS can be used to select hazard-consistent GMs at multiple intensity levels, forming the basis for establishing the EDP-IM relationship used to derive fragility. This methodology is referred to as Multiple-Stripe-Analysis or MSA (Jalayer, 2003).

One alternative to MSA is incremental dynamic analysis (IDA) (Vamvatsikos and Cornell, 2002), where instead of having different records at each stripe we have a single suite of records that is selected and then scaled incrementally to several ground motion intensities. While IDA might be useful for several applications, it does not enforce hazard consistency and hence can lead to biased fragility estimates (e.g., Kohrangi et al., 2017).

In this study, we focus on calculating fragility curves and response hazard curves of a water pump located in the reactor building of a nuclear power plant (NPP) in a site in Tuscany, Italy. We perform the analysis using two approaches: (a) MSA and CS, incorporating hazard-consistent sets of records, and (b) IDA, where hazard consistency is not explicitly enforced. In both scenarios, we explore different conditioning IMs, including spectral acceleration at 0.01s, spectral acceleration at the fundamental period T1 of the component, and average spectral acceleration (AvgSa) within a range of oscillator periods relevant for this structure. Finally, we discuss our findings with emphasis on the significance of hazard consistency and the role of conditioning IM in both analysis approaches.

2. Description of the case study

As a case study, we have selected a site in Tuscany, Italy, located on a rock with Vs30 = 1000 m/s. The Probabilistic Seismic Hazard Analysis (PSHA) calculations are carried out using the OpenQuake software (Pagani et al., 2014) and the area source model based on the European Seismic Hazard Model (ESHM20). For the hazard analysis, we utilized a logic tree with five branching sets, each one with three branches, resulting in a total of 125 different paths. We employed two ground motion models (GMMs), each with equal weights of 0.5: one from (Kotha et al., 2020) adapted by (Weatherill et al., 2020), and the other from (Lanzano et al., 2022). Figure 1a presents the site mean hazard curves for four intensity measures: Peak Ground Acceleration (PGA), Sa(0.1s), Sa(0.25s) and AvgSa within a range of oscillator periods (0.1s-0.4s). Note that the curves for the last two IMs are almost coincidental. Table 1 shows the mean magnitude (M) and distance (R) scenarios according to the disaggregation for different IMs and return periods.

The structure consists of the main containment/auxiliary building of a nuclear power plant, modeled using a simplified "masses-and-sticks" model. This model, based on the advanced AP 1000 reactor design, is implemented in the OpenSees framework (OpenSees, 2006). The model consists of three distinct "sticks" representing essential components: the Coupled Auxiliary and Shield Building (ASB), the Steel Containment Vessel (SCV), and the Containment Internal Structure (CIS). These sticks are linked at their base using rigid elements. In this study, the focus is on a specific component, a water pump, located on the top of the CIS tower. Gerontati and Vamvatsikos (2022), who employed the same AP 1000 reactor model, demonstrated that the location of the non-structural component along the height does not have a significant impact on the demand imposed on the pump by earthquake ground motions because of the stiffness and strength of the structure it is mounted on. The pump is modeled as symmetric in both the X and Y axes, using a zero-length element, and is characterized by a Hysteretic material model. We consider two cases: Model A where T_1 of the pump is 0.101 seconds and the force and displacement values at yield are 37.37 kN and 2.3 mm, respectively, and (Model B) where T_1 is 0.25s and the force and displacement values at yield are 37.37 kN and 13.9 mm, respectively. The dynamic analyses include a damping ratio of 5%. Both force and displacement exhibit

pinching factors equal to 0.5, while damage parameters are set at 0.1. The onset of failure of the component is based on ultimate displacement criteria set at the thresholds of d_u=2.9 mm and d_u=17 mm for Models A and B, respectively. Figure 1b displays the behavior of the pump (Model A) under cyclic loading.

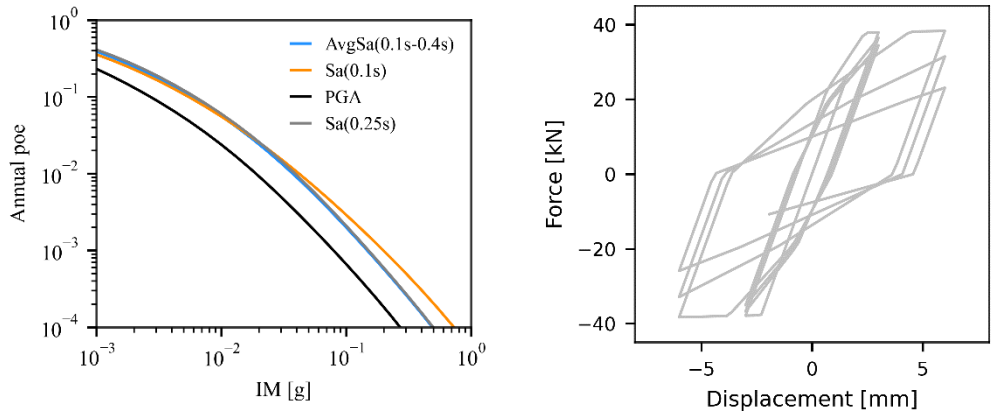

Figure 1. (a) Hazard curves for four IMs computed for the considered rock site and; (b) – Hysteretic behavior of the water pump model (Model A) under cyclic loading.

Table 1. Mean magnitude and distance (M/R in km) scenarios, based on hazard disaggregation.

Return period (yrs)	40	475	5,000	10,000	100,000
PGA	5.4/65	5.2/25	5.3/12	5.4/10	5.6/7
Sa(0.1s)	5.2/57	5.1/22	5.2/11	5.3/10	5.3/9
Sa(0.25s)	5.8/66	5.3/28	5.4/14	5.5/12	5.6/7
AvgSa (0.1s-0.4s)	5.3/59	5.3/24	5.4/13	5.5/11	5.6/8

3. Record selection

As mentioned earlier we compare the results obtained using two distinct methodologies for assessing the structural response of the water pump system under investigation. Within the framework of CS-MSA, we selected a suite of 30 records for ten intensity levels (IMLs) corresponding to return periods ranging from 40 to 100,000 years. We consider three conditioning IMs, namely Sa(0.01s), AvgSa(0.1s-0.4s) and Sa(T_1), where T_1 is 0.1s for Model A and 0.25s for Model B. For all practical purposes it is reasonable to regard Sa(0.01s) as being numerically equivalent to PGA, a commonly utilized IM in the nuclear industry (Zentner et al., 2011). We utilized Sa(0.01s) because it is the shortest oscillator period included in the Spectral accelerations' correlation matrix established by Baker and Jayaram (2008), which is needed to create the CS.

Ground motions for our investigation have been selected from widely used databases, including the Engineering Strong Motion (ESM) database (https://esm-db.eu), NGA-West2 (NGA West 2 | Pacific Earthquake Engineering Research Center (berkeley.edu)), and New Zealand Strong-Motion database (Home - GNS Science). We have focused exclusively on ground motions characterized by a minimum Vs30 value of 400 m/s. Target CS is derived using the OpenQuake software and orientation-independent measure, specifically, GMRotD50 (Boore et al., 2006) to maintain full consistency with the GMMs adopted in the hazard computations. To select "suitable" pairs of horizontal ground motion records (the vertical component is not considered in this study) we utilized the simulation approach and greedy optimization technique by (Jayaram

et al., 2011). Suitability here refers to records that collectively match, within some specified tolerance, both the mean target spectrum and the full Sa(*T*) distribution at all oscillator periods *T*. To quantify the misfit between the empirical distributions extracted from the set of selected records and the target ones, we use the sum of squared errors (SSEs) defined by Baker and Lee (2018). SSE values below 0.12 at any given period indicate an acceptable match (Iñarritu et al., 2023).

In the context of IDA, we employed a suite of 30 ground motion record pairs characterized as 'ordinary'—meaning they do not exhibit long-duration or pulse-like characteristics. These records extracted from the NGA-West2 database were selected to be consistent with the hazard of a site in Greece, for the return period of 475 years (Bakalis et al., 2018). Before the use in the IDA-based exercise, these records were scaled to the same intensity levels considered in the case of CS-MSA for the Italian rock site.

Figures Figure 2 and Figure 3 show the mean and dispersion, respectively, of the spectral ordinates of the records selected for the IML corresponding to the return period of 2500 years. These results have been derived using both the CS record selection approach and the IDA method. One can see that the mean spectrum obtained with the two methods differs substantially, with the IDA-based spectrum being higher for periods longer than 0.2 and 0.3s for the 0.01s case and the AvgSa case, respectively, and lower otherwise. For the 0.1s conditioning case, the IDA-based spectrum is always larger for all oscillator periods. Additionally, in the case of CS-selection, the dispersion is higher across the entire period range.

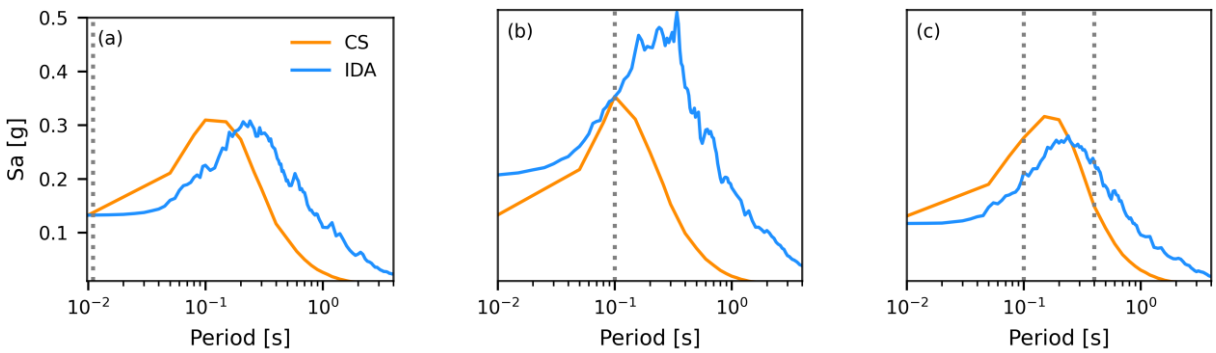

Figure 2. Mean spectra of the set of GMs selected using the CS approach and IDA approach conditioned on: (a) Sa(0.01s), (b) Sa(0.1s) and (c) AvgSa(0.1s-0.4s). All figures refer to the IML of 2500 years. The vertical dotted lines identify the conditioning period (in cases a and b) and the range of the AvgSa conditioning IM (case c).

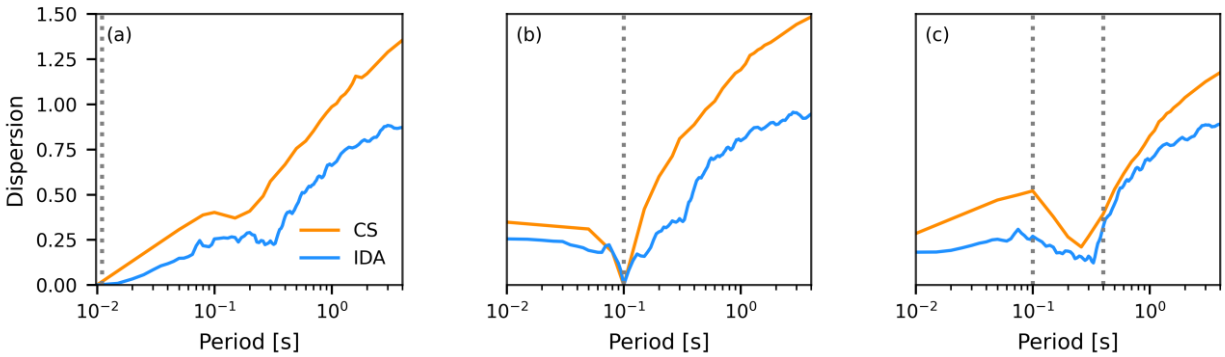

Figure 3. Dispersion of the set of GMs selected using the CS approach and IDA approach conditioned on: (a) Sa(0.01s), (b) Sa(0.1s) and (c) AvgSa(0.1s-0.4s). All figures refer to the IML of 2500 years. The dotted lines have the same meaning as in Fig. 2.

4. Results

To derive the fragility curves for the collapse case we fit a lognormal distribution to the structural demand values imposed by the fraction of ground motions leading to water pump failure. We estimate the mean and dispersion of the fragility curve using the method of moments for IDA and the maximum likelihood estimator for MSA-CS. In Figures Figure 4Figure 5, we present the resulting fragility curves for both Models A and B, considering all conditioning intensity measures (IMs) and both analysis methods. Figure 6 displays the medians and coefficients of variation (COV) for these derived fragilities.

One can see that there is a significant difference when comparing the fragility curves obtained through IDA and MSA-CS. This discrepancy underscores the critical importance of selecting ground motions that ensure hazard consistency. Furthermore, one can see that in both cases Sa(T_1) seems like the optimal choice for the conditioning IM, yielding the lowest COV of the capacity (i.e., steepest curves). However, in practical applications where multiple components with different conditioning periods need probabilistic assessment, we speculate that AvgSa may prove to be a superior choice overall. The AvgSa-based ground motions generate fragility curves with a lower COV compared to the commonly used PGA (here replaced by Sa(0.01s)), making AvgSa a favorable option for broader applicability in seismic risk assessment.

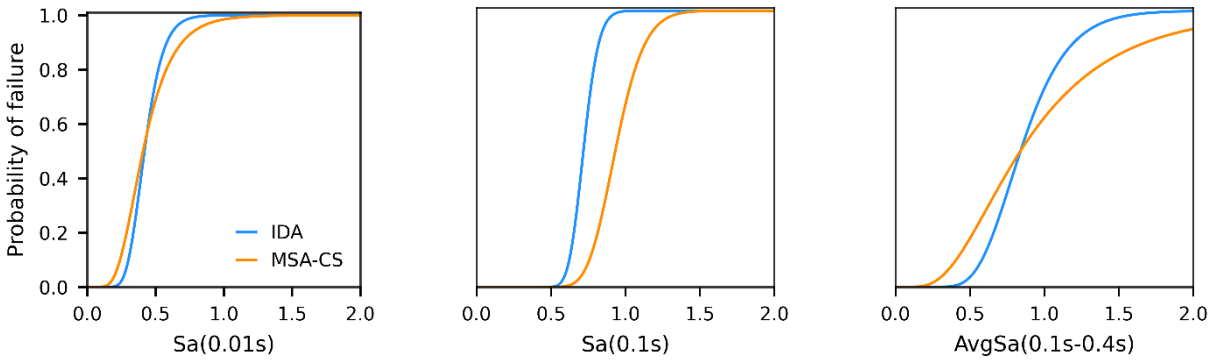

Figure 4. Fragility curves obtained using CS (orange lines) and IDA(blue lines) for Model A and different IMs.

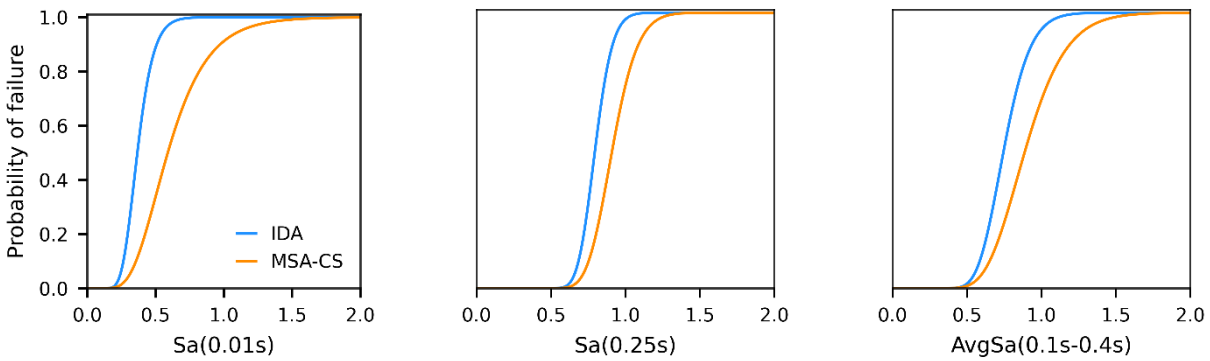

Figure 5. Fragility curves obtained using MSA-CS and IDA for Model B and different conditioning IMs.

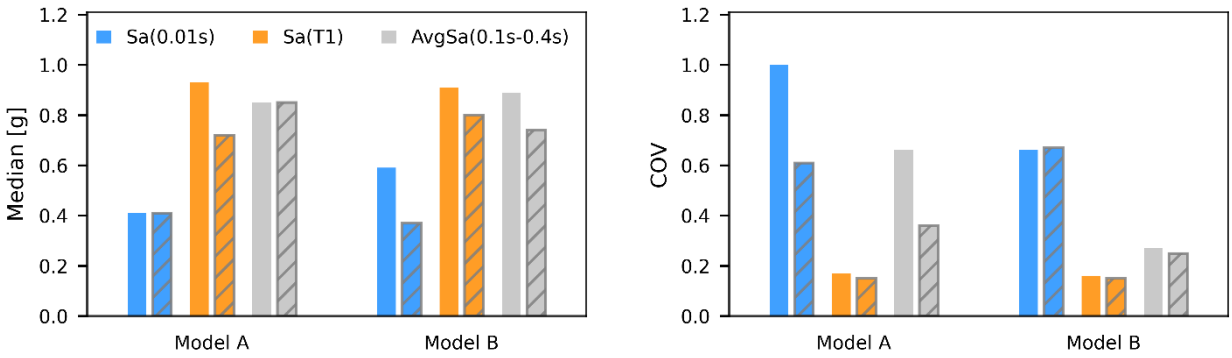

Figure 6. Median and COV of the pump capacity for Models A and B. Dashed bars refer to results obtained with IDA while solid ones refer to MSA-CS.

To quantify the seismic performance of the considered models we compute the seismic response curves, which represent the rate of exceeding different EDP levels (the EDP considered here is the maximum displacement). These curves are derived by combining the probability of exceeding a specific demand level *EDP=edp* due to the ground motion intensity *P(EDP>edp|IM=im)* with the rate of "equaling" ground motion intensity *IM* (λ_{IM}). Following the approach of Shome and Cornell (1999) *P(EDP>edp|IM=im)* can be separated into mutually exclusive collapse and non-collapse cases, resulting in the following expression:

$$\lambda_{EDP}(edp) = \int_0^{+\infty} [P(EDP > edp|\bar{C}, IM = im)(1 - P_{col}) + P_{col}]|d\lambda_{IM}(im)| \quad (2)$$

Here, $\lambda_{IM}(im)$ represents the rate of exceeding a given *IM* value *im*, P_{col} is the probability of collapse, as previously explained, and *P(EDP>edp|$\bar{C}$, IM=im)* is the probability of exceeding *EDP* value *edp* for a given *IM* value *im*, given that the structure did not collapse. The distribution of non-collapse responses is modeled using a lognormal distribution with the mean and standard deviation determined via the method of moments.

In Figure 7, we show the resulting response hazard curves for both models, obtained with MSA-CS and different conditioning IMs. One can see that there is minimal difference between these curves, suggesting that all considered IMs perform similarly. However, it's important to note that the choice of the most optimal IM may become more critical when fewer intensity levels and ground motions are considered. Conversely, Figure 8 displays response curves derived from IDA and compares them with the curve (black dotted line) calculated using MSA-CS(Sa(T$_1$)), which we consider the benchmark. We observe more pronounced differences between the various conditioning IMs compared to the MSA-CS case. Additionally, even with the most optimal conditional IM (Sa(T$_1$)), discrepancies with the benchmark are evident. For both models, the response curve obtained with AvgSa approximates the benchmark results the best.

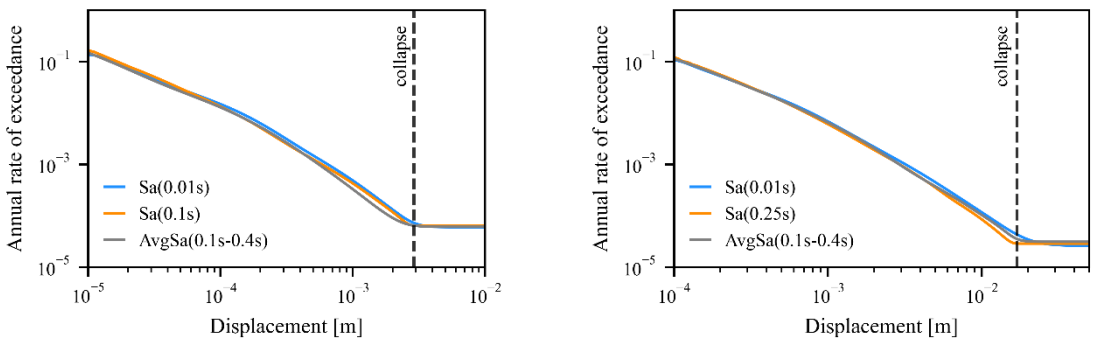

Figure 7. Response hazard curves for Model A (on the left) and Model B (on the right) using the MSA-CS method and different conditioning IMs.

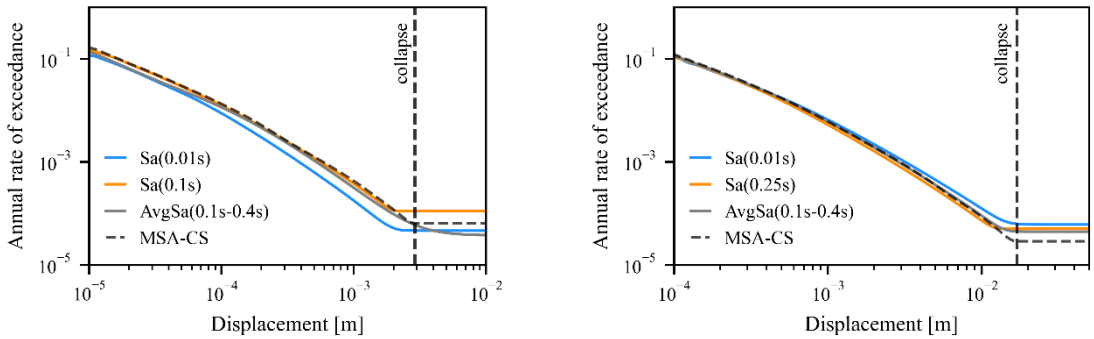

Figure 8. Response hazard curves for Model A (on the left) and Model B (on the right) using the IDA method and different conditioning IMs. Results are compared with the curve obtained using the MSA-CS method and Sa(T_1) as conditioning IM.

5. Conclusions

We utilized two methods to select ground motion records for the derivation of fragility and response hazard curves for two configurations of water pumps, one with T1=0.1s and the other with T1=0.25s, both located in the AP1000 reactor building. These methods are hazard-consistent MSA-CS and IDA, where hazard consistency is not explicitly sought and, therefore, is not guaranteed. We used different conditioning IMs: Sa(0.01s) (here considered to be equal to PGA), Sa(T1), and AvgSa(0.1s-0.4s). Our findings suggest that the optimal choice of IM remains consistent regardless of the method used. For both models, Sa(T1) consistently yields results with the lowest COV in the collapse capacity, making it the preferred choice. However, it is important to note that when evaluating the seismic risk of multiple components with varying fundamental periods mounted on the same building, Sa(T1) might not always be the most suitable choice. In such scenarios, AvgSa may emerge as a superior alternative compared to PGA, which is commonly used in the nuclear industry, as it exhibits a lower COV of the collapse capacity. AvgSa has also the practical advantage of allowing the selection of only one batch of hazard-consistent ground motions for all the response analyses concerning the different pieces of equipment.

Lastly, we observed significant disparities in fragility and response hazard curves obtained using IDA and MSA-CS. This highlights once more the critical importance of ground motion hazard consistency. In the case of MSA-CS, there are no substantial differences in response curves when different IMs are employed, in contrast to IDA, where results are more sensitive to the choice of conditioning IM. Here, response hazard curves generated with AvgSa align with the benchmark response curve obtained through MSA-CS (Sa(T1)) best.

6. Acknowledgments

We want to thank Dr. Marco Pagani for his help in the hazard analysis and Angeliki Gerontati for sharing the OpenSees model for the water pump. We are grateful to Prof. Dimitrios Vamvatsikos for his valuable suggestions and comments that improved the quality of this study.

7. References

Bakalis K, Kohrangi M and Vamvatsikos D (2018) Seismic intensity measures for above-ground liquid storage tanks. *Earthquake Engineering and Structural Dynamics* 47(9): 1844–1863. DOI: 10.1002/eqe.3043.

Baker JW (2011) Conditional mean spectrum: Tool for ground-motion selection. *Journal of Structural Engineering* 137(3): 322–331. DOI: 10.1061/(ASCE)ST.1943-541X.0000215.

Baker JW and Jayaram N (2008) Correlation of spectral acceleration values from NGA ground motion models. *Earthquake Spectra* 24(1): 299–317. DOI: 10.1193/1.2857544.

Baker JW and Lee C (2018) An Improved Algorithm for Selecting Ground Motions to Match a Conditional Spectrum. *Journal of Earthquake Engineering* 22(4). Taylor & Francis: 708–723. DOI: 10.1080/13632469.2016.1264334.

Boore DM, Watson-Lamprey J and Abrahamson NA (2006) Orientation-independent measures of ground motion. *Bulletin of the Seismological Society of America* 96(4 A): 1502–1511. DOI: 10.1785/0120050209.

Bradley BA (2010) A generalized conditional intensity measure approach and holistic ground-motion selection. (February): 1321–1342. DOI: 10.1002/eqe.

Chandramohan R, Baker JW and Deierlein GG (2016) Impact of hazard-consistent ground motion duration in structural collapse risk assessment. *Earthquake Engineering and Structural Dynamics* 45(8): 1357–1379. DOI: 10.1002/eqe.2711.

EPRI (2003) *Seismic probabilistic risk assessment implementation guide, Tech. rep., Electric Power Research Institute EPRI, Palo Alto, CA, report 1002989*.

Gerontati A and Vamvatsikos D (2022) A comparison of three scalar intensity measures for non-structural component assessment of nuclear powerplants. In: *3rd EUROPEAN CONFERENCE ON EARTHQUAKE ENGINEERING & SEISMOLOGY BUCHAREST, ROMANIA*, 2022.

Inarritu PG de Q, Šipčić N, Alvarez-Sanchez L, et al. (2023) A closer look at hazard- consistent ground motion record selection for building- specific risk assessment : Effect of soil characteristics and accelerograms ' scaling. *Earthquake Spectra* 00(0): 1–38. DOI: 10.1177/87552930231173713.

Jalayer F (2003) *Direct Probabilistic Seismic Analysis : Implementing Non-Linear Dynamic Assessments*. Stanford University.

Jayaram N, Lin T and Baker JW (2011) A Computationally efficient ground-motion selection algorithm for matching a target response spectrum mean and variance. *Earthquake Spectra* 27(3): 797–815. DOI: 10.1193/1.3608002.

Kohrangi M, Vamvatsikos D and Bazzurro P (2017) Site dependence and record selection schemes for building fragility and regional loss assessment. *Earthquake Engineering and Structural Dynamics* 46(10): 1625–1643. DOI: 10.1002/eqe.2873.

Kotha SR, Weatherill G, Bindi D, et al. (2020) *A Regionally - Adaptable Ground - Motion Model for Shallow Crustal Earthquakes in Europe*. Springer Netherlands. DOI: 10.1007/s10518-020-00869-1.

Lanzano G, Felicetta C, Pacor F, et al. (2022) Generic-To-Reference Rock Scaling Factors for Seismic Ground Motion in Italy. *Bulletin of the Seismological Society of America* (March). DOI: 10.1785/0120210063.

OpenSees (2006) Open System for Earthquake Engineering Simulation, Pacific Earthquake Engineering Research Center, University of California, Berkeley. Available at: http://opensees.berkeley.edu/.

Pagani M, Monelli D, Weatherill G, et al. (2014) OpenQuake Engine : An Open Hazard (and Risk) Software for the Global Earthquake Model. *Seismological Research Letters* 85(3): 692–702. DOI: 10.1785/0220130087.

Shome N and Cornell CA (1999) Probabilistic Seismic Demand Analysis of Nonlinear Structures. Reliability of Marine Structures. *Program Technical Report RMS-35. Standford University*.

Vamvatsikos D and Cornell CA (2002) The Incremental Dynamic Analysis and Its Application To Performance-Based Earthquake Engineering. *European Conference on Earthquake Engineering*: 10.

Weatherill G, Kotha SR and Cotton F (2020) *A Regionally-Adaptable "Scaled Backbone" Ground Motion Logic Tree for Shallow Seismicity in Europe: Application to the 2020 European Seismic Hazard Model*. Springer Netherlands. DOI: 10.1007/s10518-020-00899-9.

Zentner I, Humbert N, Ravet S, et al. (2011) Numerical methods for seismic fragility analysis of structures and components in nuclear industry - Application to a reactor coolant system. *Georisk* 5(2): 99–109. DOI: 10.1080/17499511003630512.